Proc. Indian Acad. Sci. (Chem. Sci.), Vol. 93, No. 8, December 1984, pp. 1349–1359.

Structural, magnetic and Mössbauer studies on $Mn_xFe_{3-x}O_4$ $(0 \leqslant x \leqslant 1)$

P P BAKARE, M P GUPTA, S K DATE* and A P B SINHA
Physical Chemistry Division, National Chemical Laboratory, Pune 411 008, India

MS received 11 August 1983; revised 6 April 1984

Abstract. Polycrystalline samples of $Mn_xFe_{3-x}O_4$ $(0 \leqslant x \leqslant 1)$ have been prepared following a novel route involving a reaction of desired quantities of stabilized MnO and FeO with Fe_2O_3 at high temperatures. The novel route of preparation of pure $Mn_xFe_{3-x}O_4$ precludes the presence of Mn^{3+} and Fe^{2+} ions. These samples have been characterized for their structural and magnetic properties using x-ray diffraction, Fe^{57} Mössbauer spectroscopy and bulk magnetic measurements such as initial permeability, loss factor, remanence and coercivity. All our experimental data clearly show the formation of single cubic phase over the entire range of composition. The degree of inversion in these systems decreases with increasing manganese concentration.

Keywords. $Mn_xFe_{3-x}O_4$; stabilized MnO and FeO; Mössbauer studies.

1. Introduction

Manganese-iron oxides with spinel structure are known as magnetic materials which are stable under equilibrium conditions in air. The mixed crystal series between cubic Fe_3O_4 and tetragonal Mn_3O_4 is one of the most extensively studied system. The composition and distribution of cations in the mixed system $Mn_xFe_{3-x}O_4$ are generally described by the two simple formulae (Wickham 1969),

$$Mn_x^{2+}\,Fe_{1-x}^{3+}[Fe_{1-x}^{2+}\,Fe_{1+x}^{3+}]\,O_4 \quad \text{if } x \text{ is between zero and one,} \tag{1}$$

and

$$Mn^{2+}[Fe_{3-x}^{3+}\,Mn_{x-1}^{3+}]\,O_4 \quad \text{if } x \text{ is between one and three.} \tag{2}$$

The ions enclosed in the brackets occupy octahedral sites in the spinel structure and the ions outside the brackets the tetrahedral sites. As x increases from zero to one, the manganese ions enter the lattice as Mn^{2+} ions replacing Fe^{2+} ions. However, Mn^{2+} ions prefer tetrahedral coordination and an equal number of ferric ions are therefore displaced from tetrahedral to octahedral sites. At $x = 1$, the tetrahedral sites are completely occupied by Mn^{2+} ions and further substitution of manganese for iron leads to the replacement of Fe^{3+} ions by Mn^{3+} on octahedral sites. However, the actual cation composition and distribution in mixed oxide system is not so simple and straight-forward. Even in the case of manganese ferrite $MnFe_2O_4$ (i.e. $x = 1$) disagreement is reported in the literature concerning the valency and distribution of cations (Bunget 1968). Strongly depending on the method of preparation *i.e.* starting raw materials, prefiring and sintering temperatures, ambient atmosphere quenching

* To whom all correspondence should be addressed.

processes, etc., the cations are distributed both in tetrahedral and octahedral sites leading to the compositional formula (Wickham 1969)

$$Mn^{2+}_{1-y}\,Fe^{3+}_{y}\,[Mn^{2+}_{y}\,Fe^{3+}_{2-y}]O_4$$

with the degree of inversion reported to lie between 10 and 15%. IR spectroscopic studies have also been reported (Braber 1969, 1971) for cubic and tetragonal manganese ferrites ($Mn_xFe_{3-x}O_4$) and from these results, similar compositional formula for cation valency and its distribution is obtained. In contrast differing compositional formula deduced from ^{55}Mn NMR and ^{57}Fe Mössbauer measurements has been reported as (Yasuoka *et al* 1967)

$$Mn^{2+}_{0.48}\,Fe^{3+}_{0.52}\,[Mn^{2+}_{0.06}\,Mn^{3+}_{0.46}\,Fe^{3+}_{1.02}\,Fe^{2+}_{0.46}]O_4.$$

It is then possible to explain the low magnetic moment and the high curie temperature with the canted spin structure. Between the bivalent and trivalent cations at octahedral sites, an equilibrium is postulated according to the equation

$$Mn^{2+} + Fe^{3+} \rightleftharpoons Mn^{3+} + Fe^{2+}.$$

For a long time, there was disagreement about this equilibrium. For example, the experimental data on electrical conductivity is explained by assuming such type of equilibrium on octahedral sites according to the Verwey hopping mechanism (endothermic reaction involving an energy of approximately 0·30 eV, Lotgering 1964). On the other hand, Sawatzky *et al* (1969) reported the absence of any Fe^{2+} in the B sites of $MnFe_2O_4$ from their Mössbauer studies at very low temperatures (7°K) in presence of strong external magnetic field of 55 kOe. These spectra were recorded under the stringent conditions to reduce the possibility of electron hopping and permit resolution of Fe^{2+} and Fe^{3+} subspectra. Since the Mössbauer spectra provides no evidence of Fe^{2+} ions on octahedral sites in $MnFe_2O_4$, a canted spin arrangement for Mn/Fe ions at both the sites is proposed, as reported earlier in the introduction. In fact, Enz (1958) has proposed very complicated cation distribution (Mn^{3+}, Mn^{2+}, Fe^{3+} and Fe^{2+} at both A and B sites). The various transitions will then be responsible for the electrical conductivity, effect on disaccommodation factor, magnetic relaxation and blocking of domain walls.

In summary, table 1 is the compiled experimental data related to cation distribution, hyperfine fields, NMR frequencies, magnetic moments at tetrahedral and octahedral sites reported over the last twenty years. It is clearly seen that observed differences in the various parameters of $MnFe_2O_4$ are attributable to different methods of preparation *i.e.* starting raw materials, sintering temperature and atmosphere, time of annealing, etc. followed by various workers.

A systematic study of pure and substituted manganese ferrite $Mn_xFe_{3-x}O_4$ ($0 \leqslant x \leqslant 1$) is desirable and therefore undertaken with a view to get better understanding of its complex nature. In this communication we report our structural, magnetic and Mössbauer effect measurements done for varying Mn concentration.

2. Experimental

2.1 *Preparation of highly pure Fe_3O_4 and $MnFe_2O_4$*

Pure Fe_3O_4 was prepared in the usual way of reacting Fe_2O_3 and $Fe_{(1-x)}O$ ($x < 0{\cdot}1$) in a closed system, details being given in our earlier work (Deshpande and Murthy 1981).

Table 1. Cation distribution/hyperfine field analysis in $MnFe_2O_4$.

	H_n (A) (kOe)	H_n (B) (kOe)	H_n (av) (kOe)	$n(A)/n(A)+n(B)$
Hrynkiewicz *et al* (1965) (80 K)	—	—	516	—
Wieser *et al* (RT) (1966)	470±25	450±25	—	—
Sawatzky *et al* (1967) (RT)	480±5	430±10 field distribution	—	0·12
König (1971) (80 K)	518±4	508±8	425 (RT)	0·15
Ligenza *et al* (1981) (4·2 K)	511±2	Field disat B site	—	—
Gupta and Mendiratta (1977)	475±2	458±1	—	—
Present results (RT)	448±5	422±10	—	0·13
For comparison:				
Yasuoka *et al* (1967) (NMR data)	551 Mc/sec	525 Mc/sec	—	0·10
Ligenza *et al* (1978) (Neutron diffraction data)	μ_A(293 K)=4·13; μ_B(293 K)=3·18 μ_A(85 K)=4·40; μ_B(85 K)=3·95 μ_A(4.2 K)=4·66; μ_B(4.2 K)=4·05			0·07

n(A) = intensity of Fe^{3+} at A site; n(B) = intensity of Fe^{3+} at B site.

$MnFe_2O_4$ is usually prepared by either conventional ceramic technique (Reick and Driessens 1966; Sawatzky *et al* 1969) or from coprecipitation from aqueous solution (Wickham 1969). It has been observed that the undesired concentration of Fe^{2+} and Mn^{3+} ions is present in the lattice resulting in low resistivity and low magnetic moment. In contrast, we have successfully prepared $MnFe_2O_4$, free from Mn^{3+} and Fe^{2+}, by using a novel method described earlier by Murthy *et al* (1978, 1979). Details of the experimental procedure followed in the preparation of $MnFe_2O_4$ and Fe_3O_4 are identical and described earlier by Deshpande and Murthy (1981) and Deshpande *et al* (1982).

2.2 *Mixed series-$Mn_xFe_{3-x}O_4$*

Mixed crystal series of $Mn_xFe_{3-x}O_4$ with x = 0·2, 0·4, 0·6 and 0·8 have been prepared following the same procedure in three different batches under identical conditions. All these samples are homogeneous, seen clearly from scanning electron microscopic studies.

2.3 *X-ray diffraction*

X-ray diffractograms were recorded with Philips PW 1730 x-ray generator using CuK_α radiation. All the specimens were of single cubic phase. Lattice parameter of the cubic phase were determined for each concentration in $Mn_xFe_{3-x}O_4$ series.

2.4 *Initial permeability and loss factor*

Both the initial permeability and the loss factor were determined at room temperature by measuring inductance and Q-factor using General Radio's GR 1608A impedance bridge. To measure these quantities, the toroids were insulated by covering them with cellophane tape and the enamelled copper wire was wound around it. The inductance

was measured by applying a series of ac voltages between the terminals of the copper winding. Using the standard formulae

$$\mu_i = \frac{L\,(\text{in mH}) \times 10^6}{4{\cdot}6\,N^2 \times \text{thickness (in cm)} \log \text{OD/ID}}$$

where N = number of turns of the windings and loss factor = $(1/\mu_i Q)10^{-6}$ the initial permeability and the loss factor were calculated.

2.5 *Measurement of B_r and H_c*

Remanence (B_r) and coercivity (H_c) were read directly on the B–H curve of the $Mn_xFe_{3-x}O_4$ samples traced using hysteresisgraph of Walker Scientific Inc. USA model MH-1020. Two windings—primary and secondary—were provided with enamelled copper wire on the toroids in a similar fashion as described in the permeability measurements. The ratio of primary to secondary windings was kept 1:4 as required by the instrument. The hysteresis loop was traced by connecting the wound toroid to the terminals on the test system for soft ferrites which is connected to automatic X-Y recorder. Sample was magnetized initially with a small magnetic field which was slowly increased to saturation and then reversed so as to trace the demagnetization curve and finally a complete hysteresis loop. The intercepts along the X (negative) and Yaxis give directly the magnitude of H_c and B_r respectively.

2.6 *Mössbauer spectra*

Mössbauer spectra of these mixed system $Mn_xFe_{3-x}O_4$ for all concentrations of x were recorded with a conventional constant acceleration electromechanical drive coupled to ND 100 multichannel analyser operating in time mode. A 5 mC Rh: ^{57}Co source was used to record the spectra at room temperature. A metallic iron foil (25μ thick) was used to calibrate the spectrometer and all isomer shifts were measured with respect to that of the metallic iron absorber. The hyperfine (hf) interaction parameters were computed using an iterative least squares 'MOSFIT programme adopted to ICL 1409S computer'.

3. Results and discussion

3.1 *X-ray diffraction studies*

As indicated earlier, all the polycrystalline samples were subjected to x-ray diffraction analysis. The x-ray diffractograms have clearly indicated the formation of single phase spinel after the careful and extensive intensity analysis. No traces of either iron rich or manganese rich phases in rock-salt structure have been observed in XRD patterns. The derived cubic lattice parameters for various concentrations of manganese in $Mn_xFe_{3-x}O_4$ show a smooth linear variation. The lattice parameter $a = 8{\cdot}393 \pm 0{\cdot}005$ Å for Fe_3O_4 increases linearly with increasing x. At $x = 1$ i.e. $MnFe_2O_4$, the lattice parameter $a = 8{\cdot}509 \pm 0{\cdot}005$ Å (figure 1). Similar variation has also been reported by Wickham (1969) and Cervinka *et al* (1970). A linear increase in the cubic lattice parameter is expected if one assumes that Mn^{2+} ions are replacing iron ions (Fe^{3+}) both at tetrahedral and octahedral sites since Mn^{2+} ions (0·80 Å) have a large Goldschmidt ionic radii compared to that of Fe^{3+} ions (0·53 Å).

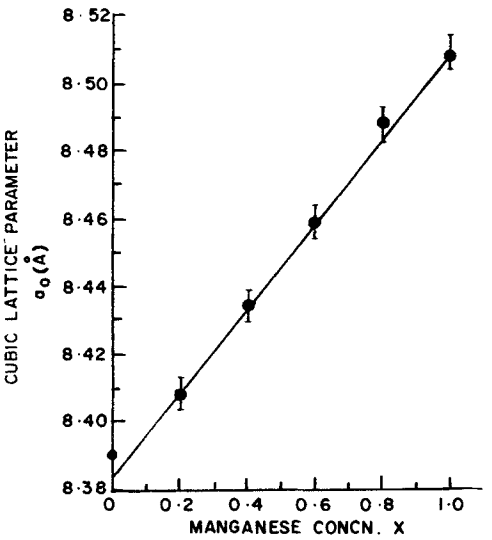

Figure 1. Cubic lattice parameters a_0 *vs* manganese concentration, x in $Mn_xFe_{3-x}O_4$.

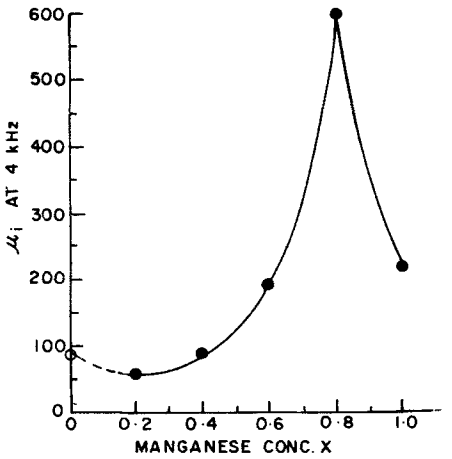

Figure 2. Initial permeability μ_i at 4 kHz *vs* manganese concentration, x in $Mn_xFe_{3-x}O_4$.

3.2 *Magnetic measurements*

Permeability of $Mn_xFe_{3-x}O_4$ increases with increasing value of x from 0·2 to 0·8 (55·57 to 599) and then suddenly drops down at $x = 1$ (219) giving rise to a peak at $x = 0{\cdot}8$ in the curve μi *vs* x as shown in figure 2. This can be explained on the basis of the effect of substitution of Mn^{2+} in $MnFe_2O_4$ by Fe^{2+} to a small extent as it serves to minimize the magnetostriction in the ferrite. This is because ferrous ferrite has a large positive magnetostrictive constant ($+40 \times 10^{-6}$) while manganous ferrite has a much smaller negative magnetostriction (-5×10^{-6}) and the stress anisotropy is minimized by making mixed ferrites with magnetostrictive constants of opposite signs blended in

such proportions as to neutralize the effects of each other. At the same time, presence of iron in two valency states however, results in a certain amount of electrical conductivity due to electron hopping and consequently increase in its loss factor due to eddy current losses. This has been confirmed by our results of loss factor measurements wherein it shows an increase from 166×10^{-6} to 1499×10^{-6} for $x = 1$ to 0·2 and is shown in figure 3 of loss factor *vs* x.

Even though importance is not given for remanence (B_r) and coercivity (H_c) in soft ferrites, we attempted to get these parameters from the hysteresis loops (figure 4). The values of B_r and H_c are given in table 2. We observed in figure 5 a nearly linear behaviour of Br which increases with increasing x. On the other hand, the coercivity decreases with increasing x except for composition $x = 0{\cdot}2$ due to its high permeability

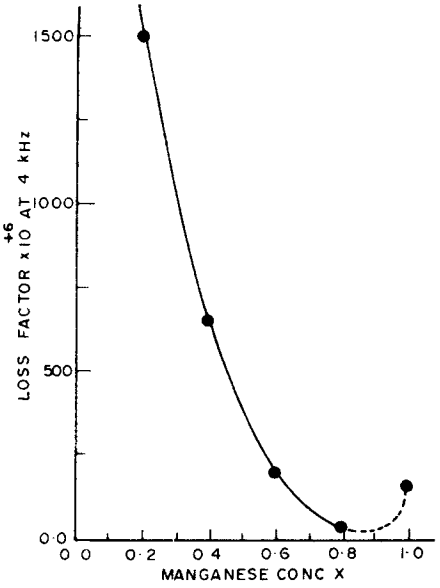

Figure 3. Loss factor $\tan \delta/\mu_i$ at 4 kHz *vs* manganese concentration, x in $Mn_xFe_{3-x}O_4$.

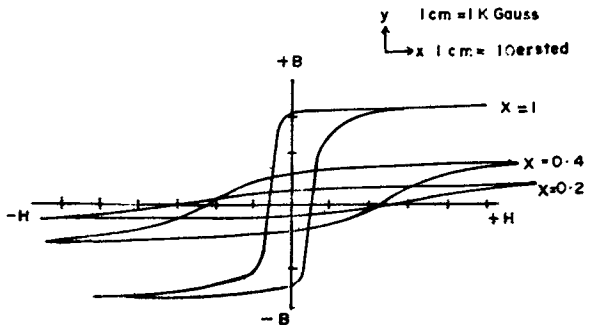

Figure 4. Hysteresis loops for three concentrations of manganese in $Mn_xFe_{3-x}O_4$ ($x = 0{\cdot}2, 0{\cdot}4, 1$).

Table 2. Magnetic properties, density and lattice parameter.

	$Mn_xFe_{3-x}O_4$ x = Manganese concn.					
	0·0	0·2	0·4	0·6	0·8	1·0
Remanence B_r (kGauss)	—	0·30	0·70	1·15	1·25	2·25
Coercivity H_c (Oe)	—	2·6	1·95	1·35	0·40	0·55
Initial Permeability μ_i at 4 kHz	—	55	88	191	599	219
Loss factor tan $\delta/\mu_i \times 10^6$ at 4 kHz	—	1499	654·6	202	45·2	166
Density (g/cc)	4·02	4·427	4·018	4·05	4·476	4·03
Cubic lattice parameter $a_0 \pm 0{\cdot}005$ (A)	8·393	8·409	8·434	8·459	8·488	8·509

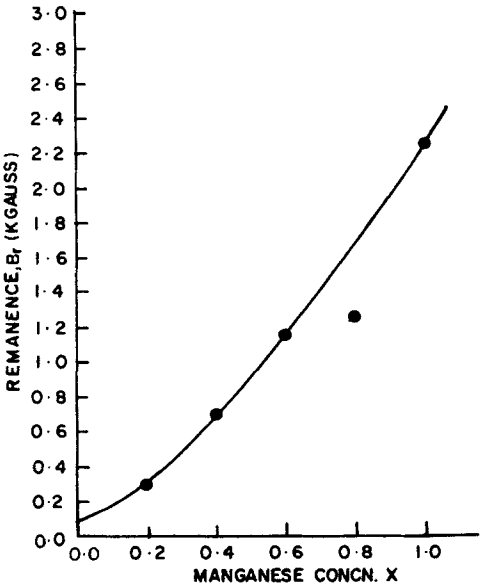

Figure 5. Remanence B_r *vs* manganese concentration, x in $Mn_xFe_{3-x}O_4$.

(figure 6). This is expected as Fe_3O_4 is known to have high coercivity and low B_r compared to $MnFe_2O_4$.

3.3 *Mössbauer results*

Figure 7 shows the typical Mössbauer spectra recorded at room temperature for various compositions of $Mn_xFe_{3-x}O_4$ where $x = 0$ (i.e. Fe_3O_4), 0·2, 0·4, 0·6, 0·8 and 1 (i.e. $MnFe_2O_4$). Figure 7a clearly shows the hyperfine (hf) split spectrum with characteristic parameters attributable to Fe_3O_4. These parameters are H_n (A) = 485 $\pm$ 5 kOe, H_n (B) = 453 $\pm$ 5 kOe, ΔE_Q (A) = 0·10 $\pm$ 0·04 mm/sec, ΔE_Q (B) = $-$0·08 $\pm$ 0·04 mm/sec, IS (A) = 0·22 $\pm$ 0·02 mm/sec, IS (B) = 0·60 $\pm$ 0·02 mm/sec. These values are in excellent agreement with those reported earlier (MEDI 1974, Deshpande *et al* 1982) and are particularly significant since Fe_3O_4 was prepared by a new method

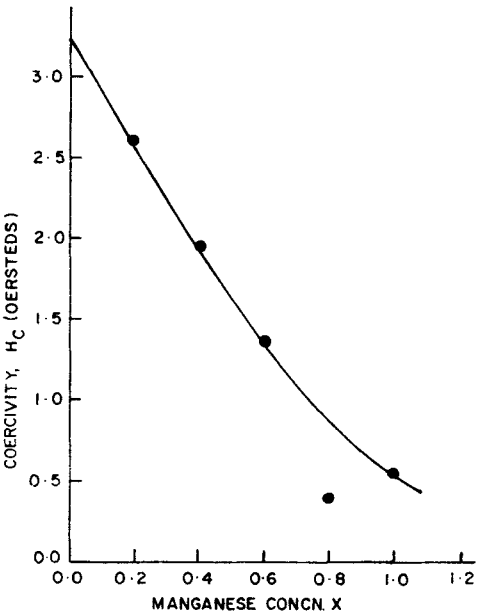

Figure 6. Coercivity H_c *vs* manganese concentration, x in $Mn_xFe_{3-x}O_4$.

(Deshpande and Murthy 1981), which is also followed in preparing other compositions in the series $Mn_xFe_{3-x}O_4$. Mössbauer spectra for the other members of the series are shown in figures 7(b) to (f). It is clearly seen that effect of manganese ions incorporating preferentially at tetrahedral sites is quite different from that reported in the case of $Zn_xFe_{3-x}O_4$ (Deshpande *et al* 1982). The various parameters such as hyperfine fields, at A and B sites, isomer shifts, quadrupole splittings, linewidths and the degree of inversion were computed and are listed in table 3. As the manganese concentration increases, the hf field at the tetrahedral site decreases very slowly while hf field at the octahedral site decreases from 458 kOe ($x = 0{\cdot}4$) to 442 kOe ($x = 0{\cdot}8$) (figure 8). At the same time, the octahedral Fe^{3+} ions show very large linewidths bordering close to those observed in case of 'electron hopping' processes occurring in other substituted ferrites. For low concentration of $x = 0{\cdot}2$, it was found difficult to fit the experimental data to the MOSFIT analysis due to broad non-Lorentzian shape. Since it has been earlier reported that there is no possibility of Fe^{2+} ions being present in $MnFe_2O_4$, we did not attempt to fit the spectra for the intermediate composition to three or four subspectra such as octahedral Fe^{3+} and Fe^{2+}, tetrahedral Fe^{3+} and Fe^{2+}, suggested by Enz (1958). Moreover, the spectra have been recorded at room temperature, it is not possible to resolve all these subspectra. For $x = 1$, the Mössbauer spectrum show well-defined hf split pattern, the hf parameters are in agreement with those reported in literature (table 1). Even though we do not have direct evidence to reject the cation distribution suggested by Yasuoka *et al* (1967) on the basis of ^{55}Mn NMR and ^{57}Fe Mössbauer results, we feel that due to our stringent preparatory conditions (*i.e.* stabilization of MnO and FeO), Mn^{3+} and Fe^{2+} will not be formed as the part of the

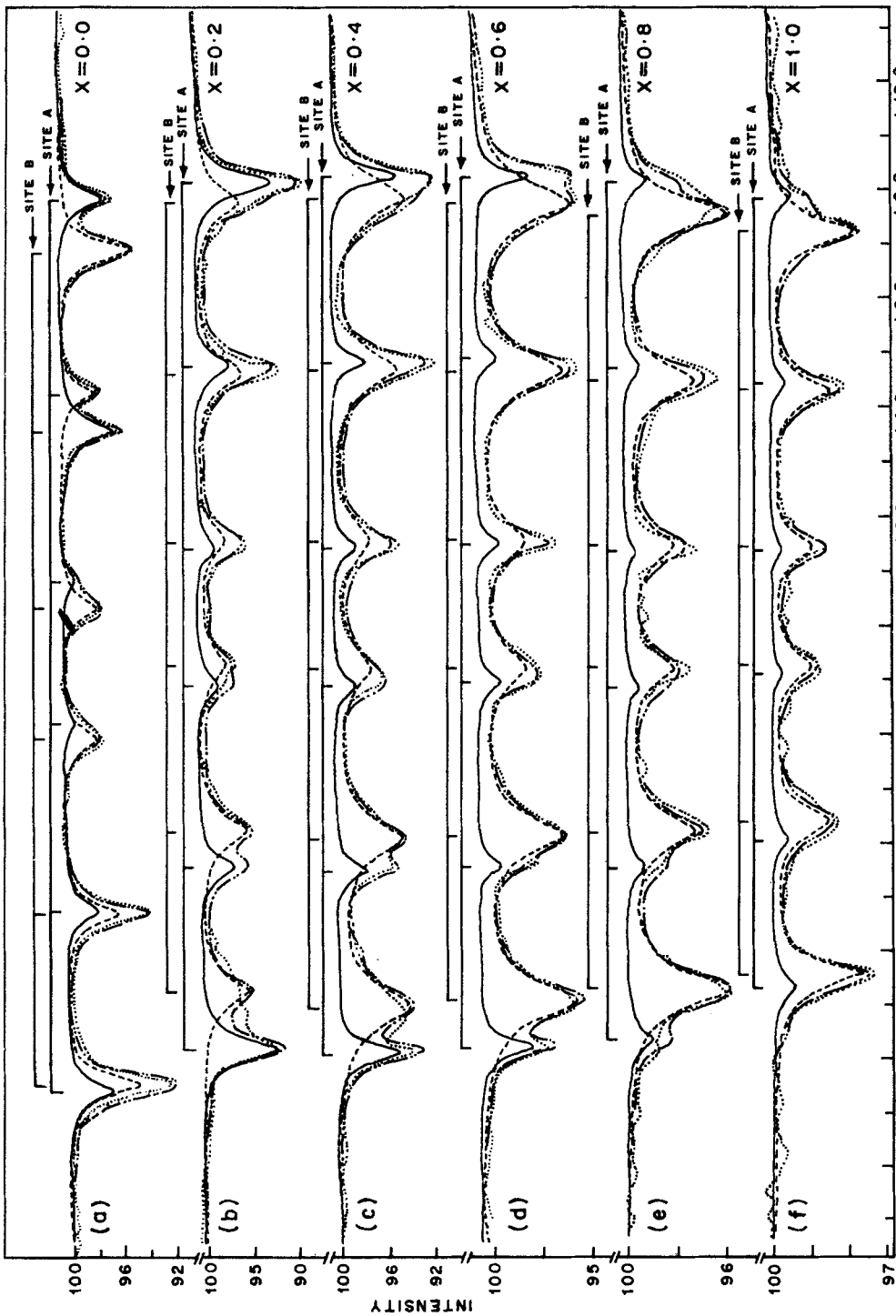

Figure 7. Mössbauer spectra of $Mn_xFe_{3-x}O_4$ at room temperature, (a) $x = 0{\cdot}0$, (b) $x = 0{\cdot}2$, (c) $x = 0{\cdot}4$, (d) $x = 0{\cdot}6$, (e) $x = 0{\cdot}8$, (f) $x = 1{\cdot}0$.

Table 3. Mössbauer parameters.

$Mn_xFe_{3-x}O_4$ Manganese conc x =	Site	IS (w.r.t. nat. iron) ±0·02 (mm/sec)	ΔEQ ±0·04 (mm/sec)	Γ ±0·02 (mm/sec)	H_n ±5 (kOe)	Inversion (%)
0·0	A	0·22	−0·10	0·39	485	32
	B	0·60	−0·08	0·44	453	
0·2	Broad non Lorentzian spectrum					
0·4	A	0·25	−0·02	0·34	495	27
	B	0·51	−0·02	0·87	458	
0·6	A	0·30	−0·02	0·32	494	17
	B	0·48	−0·03	0·86	451	
0·8	A	0·25	−0·14	0·43	490	15
	B	0·43	−0·08	0·79	442	
1·0	A	0·44	−0·33	0·45	448	13
	B	0·41	−0·04	0·63	422	

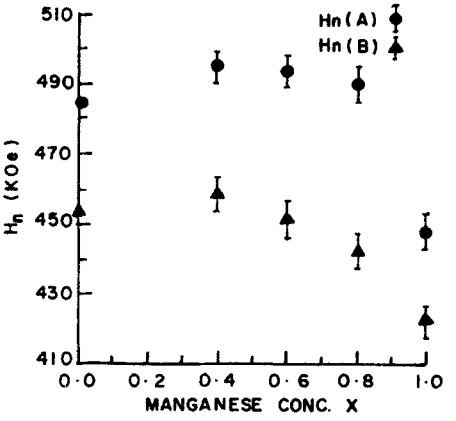

Figure 8. Hyperfine fields H_n (kOe) at A and B sites in $Mn_xFe_{3-x}O_4$.

lattice. In fact, detailed calculations by Lotgering (1964) has clearly represented this distribution by an equilibrium

$$Mn^{2+} + Fe^{3+} \rightleftharpoons Mn^{3+} + Fe^{2+}.$$

Using all other available data, the cation distribution incorporating only Mn^{2+} and Fe^{3+} is envisaged and can be written as

$$Mn^{2+}_{0\cdot74}\, Fe^{3+}_{0\cdot26}\, [Mn^{2+}_{0\cdot26}\, Fe^{3+}_{1\cdot74}]O_4.$$

It is clearly seen from the Mössbauer spectra and also from the derived hyperfine parameters that only Fe^{3+} ions are occupying both tetrahedral and octahedral sites. There is no evidence of Fe^{2+} ions occupying octahedral/tetrahedral sites resulting in broadening of the subspectra. With increasing concentration of Mn, the degree of inversion in $Mn_xFe_{3-x}O_4$ system decreases appreciably from nearly 32% (x = 0·0) to

13% ($x = 1{\cdot}0$). The decrease in the degree of inversion clearly indicates that the tetrahedral Fe^{3+} ions are being replaced by Mn^{2+} ions leading to the formation of $MnFe_2O_4$.

Acknowledgement

The authors are grateful to Dr C E Deshpande for his invaluable help in experimental work and for many useful discussions. Thanks are due to Mr J S Gujral for assistance in recording x-ray diffractograms.

References

Braber V A M 1969 *Phys. Status Solidi.* **33** 563
Braber V A M 1971 *J. Phys. Chem. Solids* **32** 2181
Bunget I 1968 *Phys. Status Solidi.* **28** K39
Cervinka L, Hosemann R and Vogel W 1970 *Acta Crystallogr.* **A26** 277
Deshpande C E, Date S K, Gupta M P and Murthy M N S 1982 *Indian Acad. Sci. (Chem. Sci.)* **91** 377
Deshpande C E and Murthy M N S 1981 *Bull. Mater. Sci.* **3** 261
Enz U 1958 *Physica* **24** 609
Gupta R G and Mendiratta R G 1977 *J. Appl. Phys.* **48** 845
Hrynkiewicz A Z, Kulgawczuk D S and Tomala K 1965 *Acta Phys. Pol.* **28** 423
Konig U 1971 *Solid State Commun.* **9** 425
Ligenza S 1978 *Phys. Status Solidi.* **b86** 635
Ligenza S 1981 *Phys. Status Solidi.* **6105** 353
Lotgering F K 1964 *J. Phys. Chem. Sol.* **25** 95
Lotgering F K and Van Diepen A M 1973 *J. Phys. Chem. Sol.* **34** 1369
Mössbauer effect data index 1974 (eds.) J G Stevens and V E Stevens (New York: Plenum Press) p. 85
Murthy M N S, Deshpande C E and Shrotri J J 1978 *Proc. Indian. Acad. Sci. (Chem. Sci.)* **A87** 49
Murthy M N S, Deshpande C E, Bakare P P and Shrotri J J 1979 *Bull. Chem. Soc. Jpn.* **52** 571
Rieck G D and Driessens F C M 1966 *Acta Crystallogr.* **20** 521
Sawatzky G A, Van Der Woode F and Morrish A H 1967 *Phys. Lett.* **A25** 147
Sawatzky G A, Van Der Woode F and Morrish A H 1969 *Phys. Rev.* **187** 747
Wickham D G 1969 *J. Inorg. Nucl. Chem.* **31** 313
Wieser E, Meisel W and Kleinstuk 1966 *Phys. Status Solidi.* **16** 129
Yasuoka H, Hirai A, Shinjo T, Kiyama M, Bando Y and Takada T 1967 *J. Phys. Soc. Jpn.* **22** 147